

PAPER • OPEN ACCESS

Optimization of a surface wave elastography method through diffraction and guided waves effects characterization

To cite this article: G A Grinspan *et al* 2016 *J. Phys.: Conf. Ser.* **705** 012014

View the [article online](#) for updates and enhancements.

Related content

- [Elastography Using Graph Cut Algorithm](#)
Naoto Akazawa, Kan Okubo and Norio Tagawa
- [Identification of viscoelastic properties by magnetic resonance elastography](#)
Nobuyuki Higashimori
- [Imaging of dose distributions using polymer gels based on radiation induced changes in stiffness](#)
Remo A Crescenti, Jeffrey C Bamber, Assad A Oberai *et al.*

Recent citations

- [Surface wave elastography: device and method](#)
Nicolás Benech *et al*



IOP | ebooks™

Bringing you innovative digital publishing with leading voices to create your essential collection of books in STEM research.

Start exploring the collection - download the first chapter of every title for free.

Optimization of a surface wave elastography method through diffraction and guided waves effects characterization

G A Grinspan¹, S Aguiar², N Benech³

¹Sección Biofísica, Facultad de Ciencias, Universidad de la República, Montevideo, Uruguay

²Instituto de Ensayo de Materiales, Facultad de Ingeniería, Universidad de la República, Montevideo, Uruguay

³Laboratorio de Acústica Ultrasonora, Facultad de Ciencias, Universidad de la República, Montevideo, Uruguay

E-mail: gustavogrinspan@hotmail.com

Abstract. Soft biological tissue elasticity is a parameter whose reliable measure is relevant to many applications in fields as diverse as medicine and the agrifood industry. The ultrasonic elastography methods are often unviable to be applied to provide such solutions. In this way, the surface wave elastography (SWE) appears as a viable alternative, due its low cost, easy to use, non-invasive-destructive character as well as its ability to provide *in vivo* estimates. Previous studies have described a good correlation between the overall behavior of ultrasonic elastography and SWE, although the latter overestimates the elasticity values compared to the first. It has been suggested that this is due to the influence of certain physical effects related to the exclusive use of low frequency waves, as well as by characteristics of the experimental setup and/or medium. In this work we confirm the influence of such effects and discuss different strategies to make independent the estimations thereof. This allows achieving a good agreement between the ultrasonic reference method and SWE. Thus, SWE becomes a reliable method to estimate soft biological tissue elasticity.

1. Introduction

Elasticity is an important parameter to assess in those areas where it is relevant to infer the intrinsic mechanical state of soft solids. Some examples of soft solids include rubber, gels, agrifoods and soft biological tissues. The interdisciplinary study of the mechanical properties of this type of medium, allows addressing complex problems of different areas of knowledge, with potential applications in different fields. For example, the elasticity of skeletal muscle is a parameter closely related to relevant factors both for the meat industry as well as for the rehabilitative medicine, such as the tenderness of meat and muscle tone, respectively.

The elastography research field has contributed greatly in recent years, providing numerous studies and methods to evaluate the Young modulus (Y) of this type of medium in a non-destructive and non-invasive way. Particularly, the transient elastography (TE) has positioned as a reference in the field of elastography. Thus, its applications have served both to determine the elasticity of soft biological tissues *in vivo* as skeletal muscle ([1], [2], [3]), or *in vitro* as agar-gelatin phantoms and meat ([4], [5]). However, the dependence between its functioning and the presence of multiple diffusers into the medium (which



originates the speckle acoustic signals), coupled with the high costs of implementation due to the requirements of its electronics, implies that the use of the ET is unviable within certain specific areas.

An alternative to ultrasonic methods has been the exclusive use of low-frequency waves. In this sense, it is possible to find works that refer to the use of surface waves (or Rayleigh waves) to determine the mechanical properties of soft solids ([6], [7], [8], [9], [10], [11], [12]). Particularly, an SWE method composed of a linear array of piezoelectric sensors, was proposed by the authors of [13] to measure the elasticity of the human brachial biceps *in vivo*. In this work are shown dispersion curves that describe how at frequencies in the order of 100 Hz and higher, the behavior of the method have a good agreement with ET, although it overestimates the elasticity values with respect to the latter. It is suggested that this could be due to diffraction and guided waves effects, being then necessary confirm the presence of such effects and to develop strategies that allow obtaining accurate estimations of elasticity.

Therefore, the objective of this work is to study in detail the impact of diffraction and guided waves effects on the SWE method proposed in [13], as well as alternatives are proposed to make independent the estimations of such effects.

2. Materials and methods

2.1. Surface wave elastography method (SWE)

The SWE involves the propagation of waves across the surface of medium, to estimate its elasticity through the study of such vibrations. In this sense, the experimental setup that composes this method is an external source (mechanical vibrator), whose frequency range is determined by the particular properties of the medium of interest. Also, depending on the specific vibrator used, this may have, or not, an attached rod to transmit the vibration to the medium. In this sense, we used a speaker with an attached piston, which generates a cycle of sinusoid with a central frequency between 50 and 250Hz. The vibration is normal to the surface, so excites mainly the vertical component of the surface waves. The wave thus generated is recorded by a linear arrangement of four piezoelectric vibration sensors, which are disposed on the surface of medium and record the vertical component of the vibration. Subsequently, an 8-channel data acquisition board (converting A/D) acquires the recorded signals and transfers them to a computer to the data processing (figure 1).

2.2. Signal processing

As we have seen previously, the method is composed by 4 sensors aligned with the exciting source. These sensors capture the acoustic vibration producing a potential difference between its terminals that is digitalized by the data acquisition board (figure 1).

From the digitized signals, the main objective of the method is to estimate the temporal delay between the signals recorded by the sensors of the linear array (figure 2a). Once the delay is estimated, as the distance d between sensors is fixed, the speed of the vibration in the medium can be obtained. The first step in the signal processing consists of applying a bandpass filter centered on the emitter frequency and a bandwidth of 30%. This procedure allows eliminating the unwanted frequencies in the signal that may affect the estimation of the surface wave speed.

The second step is to estimate the delay between consecutive signals. To do this, we used an correlation algorithm of signals based on normalized covariance between them:

$$R(j) = \frac{\sum_i (x(i) - \bar{x})(y(i+j) - \bar{y})}{\sqrt{\sum_i (x(i) - \bar{x})^2 \sum_i (y(i) - \bar{y})^2}} \quad (1)$$

In the above expression x and y represent two acoustic signals recorded by two consecutive sensors, and the values of indexes i , j represent the time (discrete because the signal is sampled at a given frequency fs). The value of j , which maximizes the value of R is the first step to estimate the shift δt between two consecutive signals: $\delta t = j/fs$. In this way the value of temporary delay that can be measured is given by discrete steps limited by the sampling frequency fs .

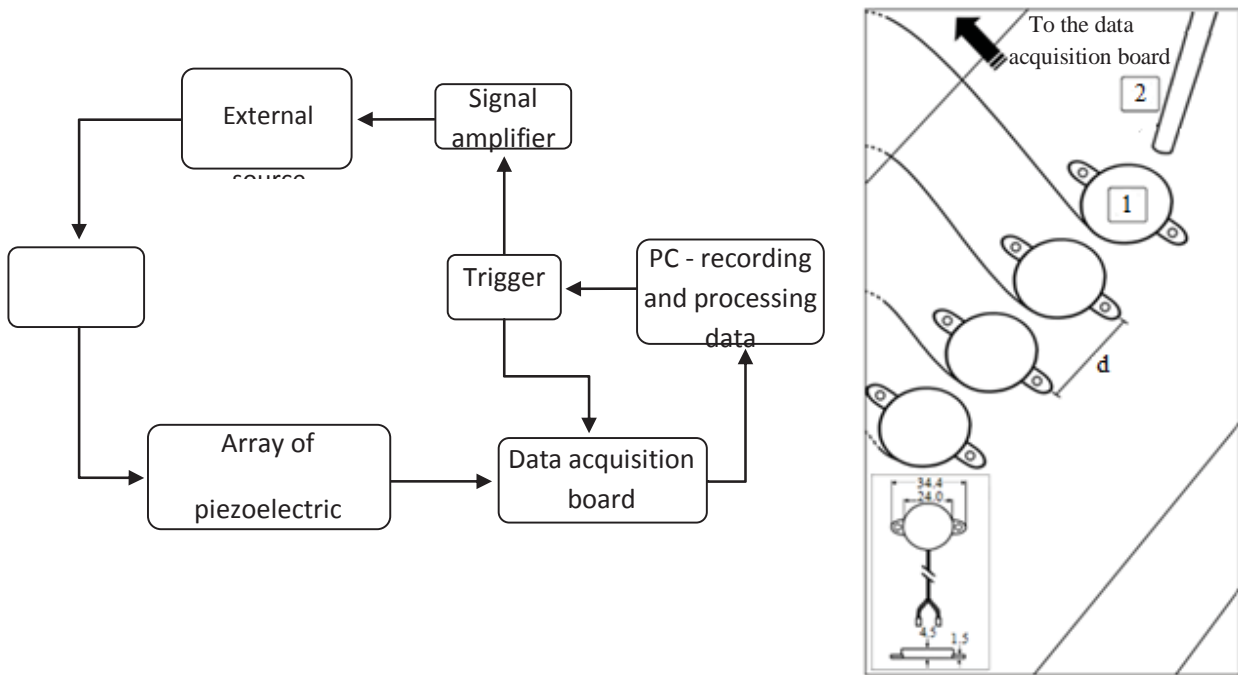


Figure 1. Flowchart of the experimental setup of SWE method and linear array of piezoelectric vibration sensors (1) aligned with the rod attached to the mechanical vibrator (2).

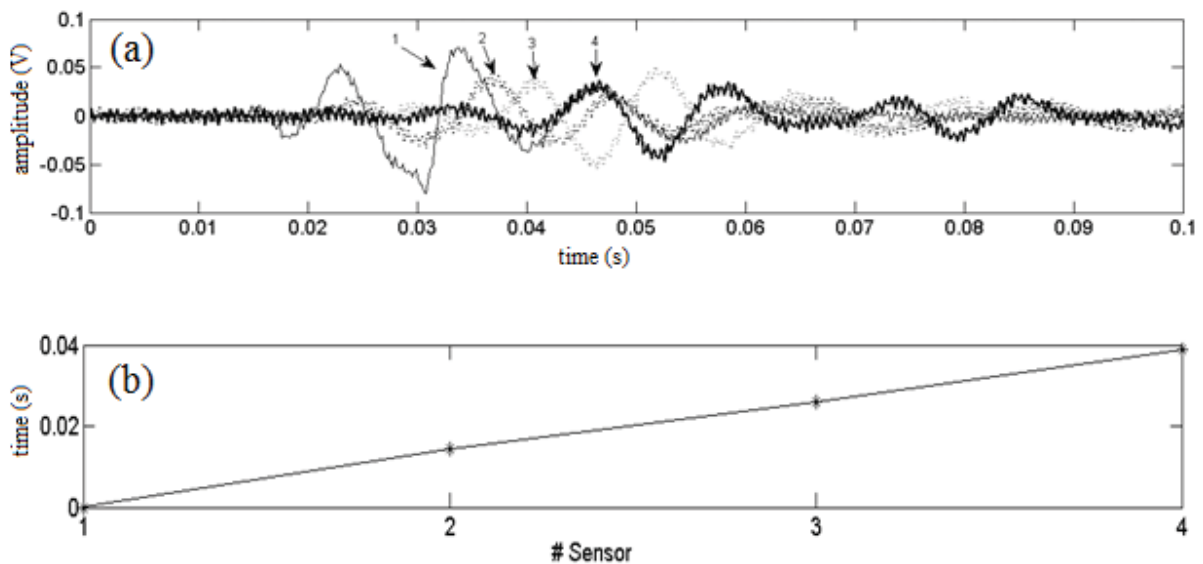


Figure 2. (a) typical signals recorded by the vibration sensors. (b) accumulative sum of the time-shift between sensors, which determines the time of arrival of surface wave to each.

To overcome this limitation, the third step in the signal processing consists of making a parabolic interpolation of the correlation coefficient R around the maximum. We chose the parabolic interpolation because it is computationally efficient. Assuming for the first sensor time 0, the final result is a vector of 4 inputs, each one with the temporary shift of the signal between sensors. The accumulative sum of these times provides the arrival time of the surface wave to each sensor (taking as origin the arrival time to the first sensor). Finally, we get a $\delta t(r)$ curve, where r represents the position (known) of each sensor (figure 4b). The next step in the signal processing is to perform a linear fit of the $\delta t(r)$ curve. The inverse of the slope of this fit is the Rayleigh surface wave speed. There is a relationship between the Rayleigh waves speed and the shear waves c_s given by the expression known as Viktorov formula [14]:

$$\frac{c_R}{c_s} = \frac{0,718 - (c_s/c_p)^2}{0,75 - (c_s/c_p)^2} \quad (2)$$

where C_p is the compression waves speed. Since in soft solids the elastic modulus of compression (λ) is much greater than the elastic modulus of shear (μ), we have that $C_p \gg C_s$. As a result we can obtain an approximate expression that relates the Rayleigh wave speed with the shear wave speed:

$$\frac{c_R}{c_s} \approx \frac{0,718}{0,75} = 0,96 \Rightarrow c_R = 0,96c_s \quad (3)$$

Therefore, and according to the fact that in soft solids the speed of shear wave is related to Young's modulus by $Y = 3\rho c_s^2$ (where ρ is the density of the medium), by measuring the speed of Rayleigh waves through the procedure described, we can finally estimate Y by:

$$Y = 3\rho(1,04c_R)^2 \quad (4)$$

2.3. Experimental setup

It was used the SWE method in different experimental conditions, with the objective of characterizing the diffraction and guided waves effects, as well as to analyze different strategies to make the estimations independent of such effects.

We perform measurements in agar-gelatin phantoms, which simulate the mechanical properties of soft biological tissues. Two phantoms were manufactured: N°1: 2.5% of gelatin, 1% agar, dimensions 12.0 x 12.0 x 4.0 cm³ (length, width and height); N° 2: 3.5% of gelatin, 1.5% agar, dimensions 12.0 x 12.0 x 4.0 cm³. Each of these phantoms were measured intact, as well as after cutting them at the middle of height, being then its dimensions 12.0 x 12.0 x 2.0 cm³. Furthermore, the phantoms were measured with different values of frequency, varying within the range of 50-160Hz.

3. Results and discussion

3.1. Experimental confirmation of the incidence of diffraction and guided wave effects

Results presented in [13] denote that the SWE is a useful elastography method to evaluate changes in the mechanical properties of soft biological tissues. However, although this version has shown characterize analogously the changes in the elasticity of brachial biceps under different situations of static load, it is appreciated that overestimates the values of C_R with respect to the real values provided by the ET (figure 7). It is suggested that this may be due to the influence of diffraction as well as geometric dispersion effects associated with guided waves.

The diffraction effect occurs when the separation between the source and the receiver is in the order of the wavelength and the source has comparable dimensions to the latter. In addition to the overestimation of velocity values, this produces a characteristic dispersive effect whereby the value of C_R decreases as

increases the frequency of the wave [15]. In this regard, figure 3 clearly reflects the impact of the diffraction effect on the experiences made with phantoms N°1 and N°2, coinciding with the frequency analysis displayed in [13] obtained from the estimates in braquial biceps. The characteristics of the experimental setup used in both cases allow us to assume a punctual source, since your radius is much less than the wavelength in soft solids at the typical frequencies (between 10 and 60 mm, depending on the speed). However, the size of the piezoelectric sensors (10mm radius) is not depreciable relative to the wavelength and the separation between them is small compared to the same. As a result, and given the reciprocity emitter/receiver of the acoustic field generated, we must consider the diffraction effects associated with the reception of waves.

The guided waves effect occurs when the height of the sample is comparable to or less than wavelength. From the analytical point of view, the effect of guided waves is more complex than the diffraction, since there are two types of modes of guided waves, and each mode has in principle several possible orders of propagation. Fortunately, in recent years it has been reported that in soft solids the predominant mode (or the only possible depending on the experimental conditions) at low frequencies is known as antisymmetric mode of order 0 or A0 [12]. This mode has an inverse dispersion condition with respect to the diffraction effect, since by increasing the frequency and/or the height of the sample, the apparent speed is higher and closer to the real speed (Figure 4). This is reflected in the results obtained with phantoms N°1 and N°2 halved by a horizontal cut (Figure 5). Compared with figures 3a and 3b, we can see the maintenance of the downward trend of the speed according to the frequency, but numerical values are lower. The downward trend is maintained because the effect of diffraction is still present and it is dominant with respect to guided waves, but the decrease of numerical values is attributable to this effect since the dispersive pattern operates in the opposite direction. From previous experiences, it can be concluded that to avoid the effect of guided waves, it is suitable to work with high-altitude samples (compared with the wavelength) or in equivalent form, increase the frequency f_0 of the surface wave. For the applications of this method, it is not feasible to modify at will the height h of the samples. Therefore, it is necessary to choose appropriately the optimal operating frequency according to the application itself.

3.2. Correction of diffraction from analytical expressions

In some particular cases it is possible to obtain an analytic expression for the diffracted wave field. For surface waves in elastic media, the authors of [16] obtained an expression for the radiation at frequency ω of a circular piston acting normally to the free surface of solid:

$$u_z(r) = \frac{ae^{i\omega t}}{\mu} \int_0^\infty \frac{J_1(aq\zeta)\sqrt{\zeta^2-1}}{F_0(\zeta)} [2\zeta^2 + \eta^2 - 2\zeta^2] J_0(\zeta r q) d\zeta \quad (5)$$

In the above expression $u_z(r)$ is the normal component of the field at distance r from the source, a is the radius of the circular piston, q is the number of wave of compression waves, η is the number of wave of shear wave normalized with respect to q , J_n is the Bessel function of order n , ζ is the variable of integration with respect to q and F_0 is the Rayleigh function:

$$F_0(\zeta) = (2\zeta^2 - \eta^2)^2 - 4\zeta^2\sqrt{\zeta^2 - \eta^2}\sqrt{\zeta^2 - 1} \quad (6)$$

Given the reciprocity emitter/receiver of the acoustic field generated, the expression (5) allows us to compute the module and the phase of the field emitted by a punctual source and received by a circular sensor of radius a , as in our experimental arrangement. Because the integral expressed in (5) has no known analytical solution in the near field, we must resort to numerical solutions to know the module and phase of the field in each sensor of the linear array at a given frequency ω . This calculation allows us to compute the apparent speed c_a according to the frequency through:

$$c_a = \frac{\omega}{k} = \omega \left(\frac{\Delta\varphi(\omega)}{\delta} \right)^{-1} \quad (7)$$

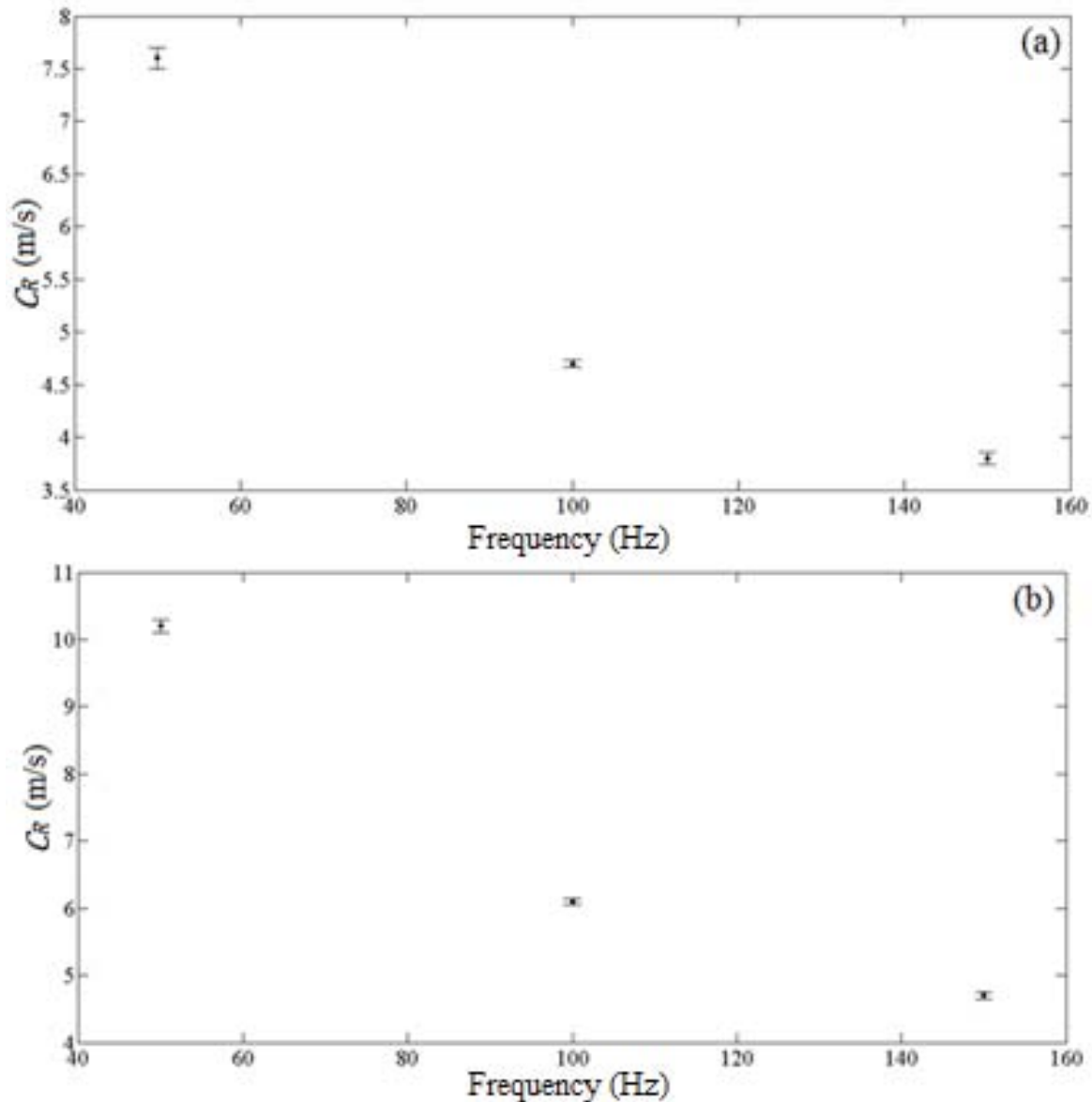


Figure 3. Dispersion curve of Rayleigh wave speed obtained in phantoms N°1 (a) and N°2 (b) at 50, 100 and 150Hz. Error bars correspond to the standard deviation on 15 measures.

where k represents the apparent number of wave, $\Delta\varphi(\omega)$ is the phase difference between the two sensors to the frequency ω and δ is the distance between them. We should note that to obtain numerically the phase difference $\Delta\varphi(\omega)$ from the expression (5), it is necessary to know the speed of the shear waves (because the shear modulus μ is present in the expression). But this is precisely the purpose of the SWE method. To find it, we propose to use an inversion algorithm based on the model of diffraction for an only experimental measure. The range of speed of the shear waves introduced into the algorithm is based on certain prior knowledge (in the case of agar-gelatin phantoms we set the range in 1-6 m/s). In this way, using the model of [16] we obtain numerically a curve $c_a(c_s)$ at a given frequency (we should note that all other experimental parameters remain fixed for a given configuration of the source and sensors). From this curve, we can then introduce the experimental result of the apparent speed and obtain the corresponding value of shear waves as shown in figure 6.

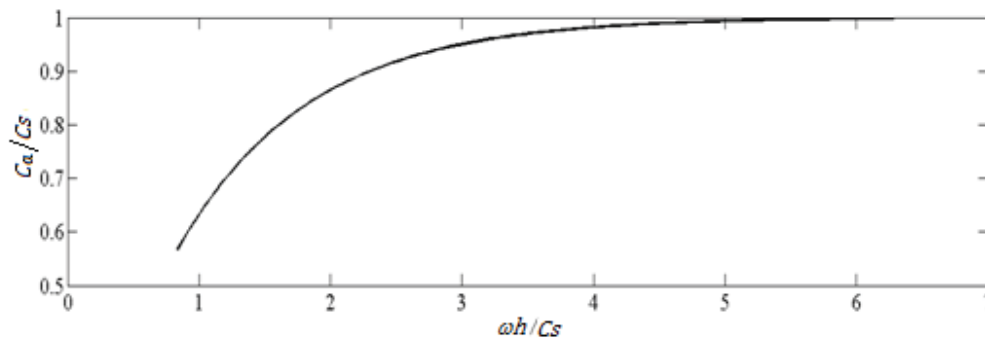


Figure 4. Dispersion curve to the $A0$ mode. c_a : apparent speed; c_s : shear waves speed; ω : angular frequency of the wave; h : sample height. It follows that the higher the variable $x = \omega h/c_s$, nearest is the apparent speed to the real speed.

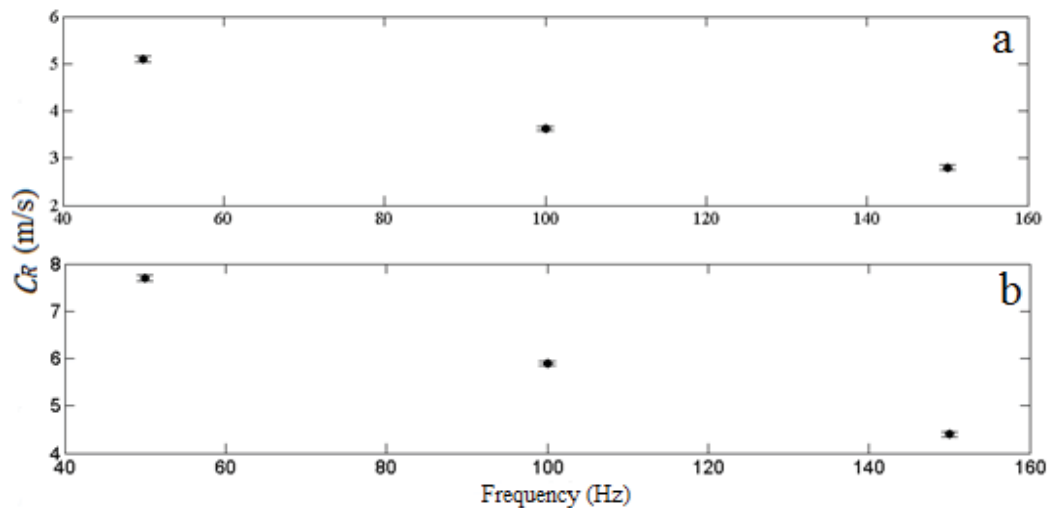


Figure 5. Rayleigh wave speed in function of frequency for phantoms N°1 (a) and N°2 (b) with $h = 2\text{cm}$. Error bars correspond to the standard deviation on 15 measures.

We perform this procedure with the experimental results of [13] for the measurement of elasticity in brachial biceps under different load conditions. The results shows a significant reduction in the diffraction effect, whereby the SWE already not overestimates the values of c_s , but on the contrary the results fit very well to the values provided by the ET (figure 7). For its part, after to perform this procedure with the experimental results obtained with gels N°1 and N°2, it is observed that our inversion algorithm retrieves the value of c_s for all frequencies in both gels (figures 8a and 8b). In this way, beyond the experimental uncertainty, the velocity values already not evidence the dispersive pattern of diffraction effect, as may be expected in an elastic solid. Likewise, if we apply the inversion algorithm to the results obtained with the phantoms N°1 and N°2 halved by a horizontal cut, we see that trend is modified with respect to figure 5, eliminating the effect of diffraction since now the speed of the Rayleigh wave increases in accordance with the increase of frequency (figures 9a and 9b). This is in agreement with the theory for guided waves taking into account the experimental conditions ($h = 2\text{cm}$). In addition, we can see that the value obtained at 150 Hz retrieves the speed value shown in figures 8a and 8b ($h = 4\text{cm}$) to the same frequency. The latter has important connotations related with avoid the effect of guided waves, since we can conclude that if we put our experimental condition for values of $x > 3$ (figure 4) it is possible to depreciate the incidence of this effect.

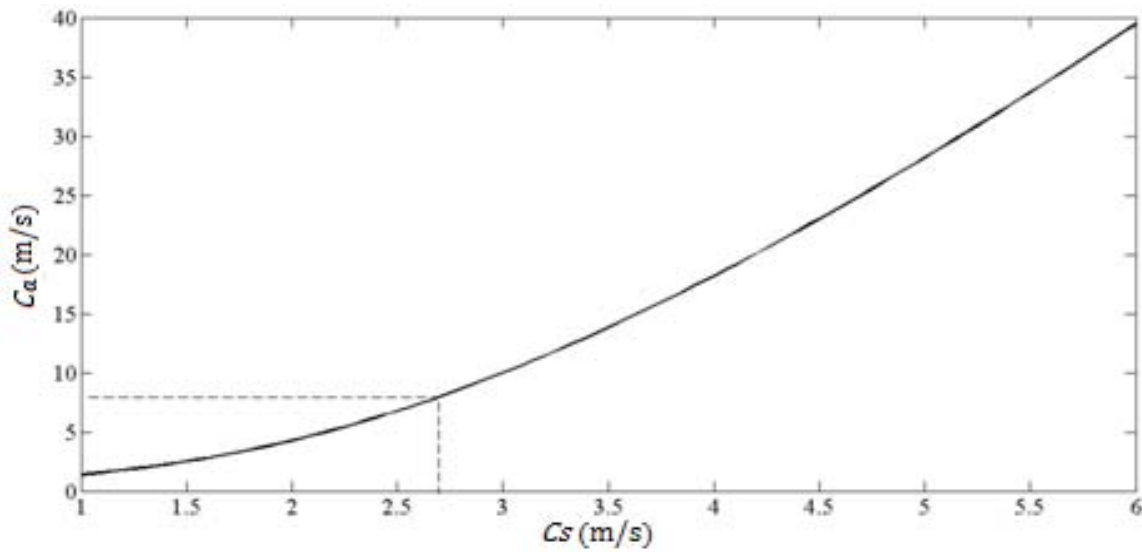


Figure 6. Apparent speed (c_a) in function of shear wave speed (c_s) for a fixed frequency (50Hz), from which we can estimate c_s knowing the c_a measured experimentally. Here we display the estimation for phantom N°1 at 50 Hz, whose estimated value is $c_s = 2.72 \text{ m/s}$.

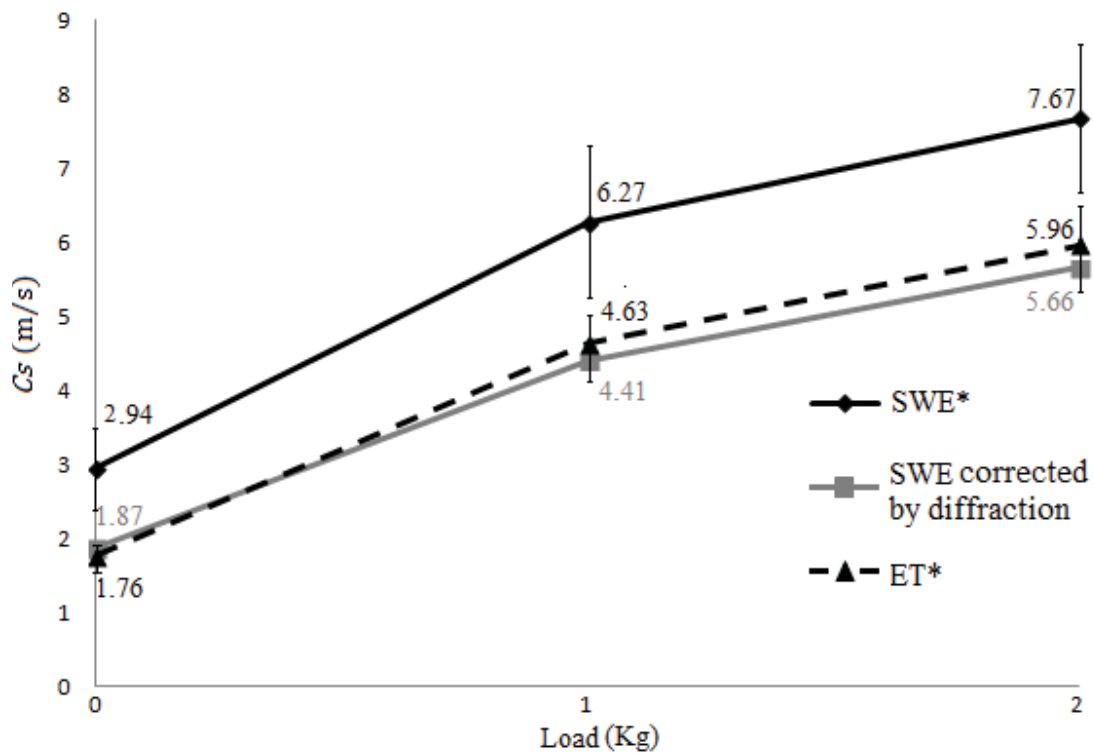


Figure 7. Numerical correction of diffraction effect applied to measurements of muscular elasticity of [13] (*).

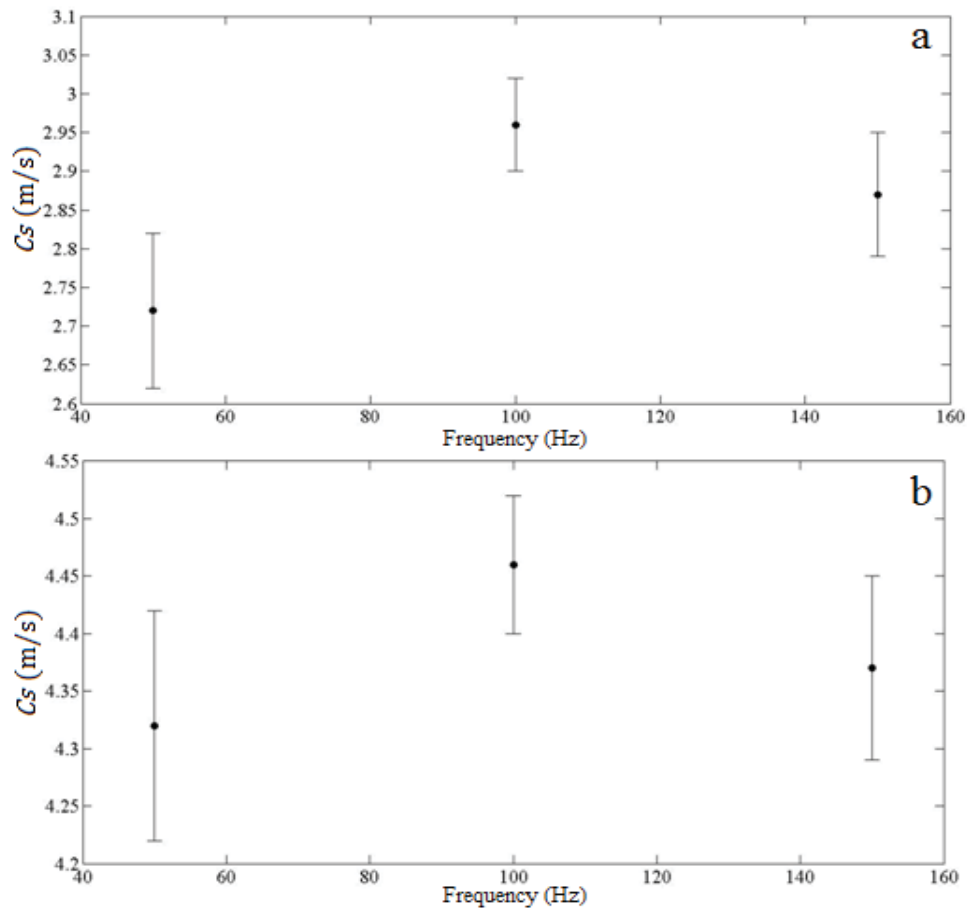


Figure 8. Shear wave speed in function of frequency for phantoms N°1 (a) and N°2 (b), corrected according to our inversion algorithm. Error bars correspond to the standard deviation on 15 measures.

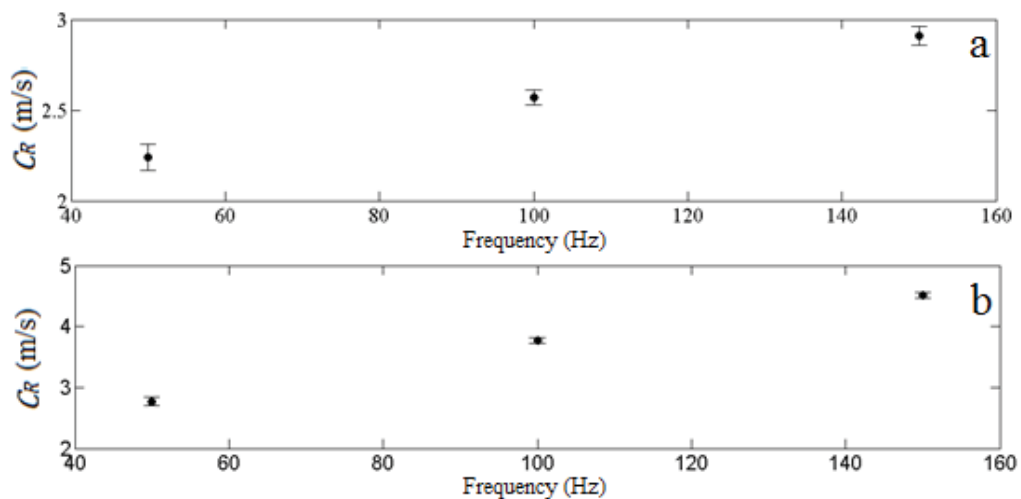


Figure 9. Rayleigh wave speed in function of frequency for phantoms N°1 (a) and N°2 (b) with $h = 2\text{cm}$, corrected according to our inversion algorithm. Error bars correspond to the standard deviation on 15 measures.

4. Conclusions

The present work shows that the SWE is a viable alternative to characterize the biomechanical properties of soft biological tissues. It has been confirmed the hypotheses proposed in [13], about that the exclusive use of low-frequency waves induces diffraction and guided waves effects. This results in an overestimation of the elasticity in relation to the ultrasonic reference methods. In this sense, the inversion algorithm proposed to correct numerically the diffraction and the criterion to depreciate the guided waves effects, have allowed achieving the independence of such effects and adjusting very well the results to the ET. However, beyond these strategies of correction are effective, are not sufficiently efficient for the applications of interest since they require a further processing of data and do not allow obtaining real-time estimates.

The non-invasive character, in vivo applicability, easy use and low cost, are features of the SWE that open up a wide spectrum in terms of their potential applications. This work represents a significant advance in what refers to the understanding of these methods, its limitations and how to overcome them. Developing strategies that allow to correct in real time the incidence of the described effects, is the key step to achieve that the SWE can offer the effective solutions that are necessary in those fields that do not have objective methods to quantifying the soft biological tissue elasticity. Rehabilitative medicine and agrifood industry (e.g. meat industry) are clear examples of the latter.

5. References

- [1] Gennisson J L, Cornu C, Catheline S, Fink M and Portero P 2005 *J. Biomech.* **38** 1543
- [2] Gennisson J L, Catheline S, Chaffai S and Fink M 2003 *J. Acoust. Soc. Am.* **114** 536
- [3] Nordez A, Gennisson J L, Casari P, Catheline S and Cornu C 2008 *J. Biomech.* **41** 2305
- [4] Benech N, Negreira C and Brito G 2012 *Elastografía ultrasónica para evaluación de la ternera de carne vacuna* (Montevideo, PROCISUR publicaciones).
- [5] Catheline S, Gennisson J L, Delon G, Fink M, Sinkus R, Abouelkaram S and Culioli J 2004 *J. Acoust. Soc. Am.* **116** 3734
- [6] Kazarov V V and Klochkov B N 1989 *Biophysics* **34** 742
- [7] Sarvazyan A, Ponomarjev V, Vucelic D, Popovic G, Vexler A 1992 *EP Patent* **0329817** B1
- [8] Courage W 2003 *US Patent* **6619423** B2
- [9] Sabra K G, Conti S, Roux P, Kuperman W A 2007 *Appl. Phys. Lett.* **90** 194101
- [10] Salman M and Sabra K G 2013 *J. Acoust. Soc. Am.* **133** 1245
- [11] Zhang X, Qiang B and Greenleaf J 2011 *Ultrasonics* **51** 157
- [12] Brum J, Gennisson J L, Nguyen T M, Benech N, Fink M, Tanter M and Negreira C 2012 *IEEE Trans. Ultras. Ferroelec. Freq. Contr.* **59** 703
- [13] Benech N, Aguiar S, Grinspan G A, Brum J and Negreira C 2012 *Proc. IEEE Ultras. Symp.* **2012** 2571
- [14] Diulesaint E and Royer 1980 *Elastic waves in solids* (New York: Wiley)
- [15] Ruiz A and Nagy P B 2002 *J. Acoust. Soc. Am.* **112** 835
- [16] Miller G and Pursey H 1954 *Proc. R. Soc. A.* **223** 521